EURASIP Journal on Wireless Communications and Networking 2004:2, 222–235


# Cochannel Interference Mitigation and Cooperative Processing in Downlink Multicell Multiuser MIMO Networks

**Hongyuan Zhang**
*Department of Electrical and Computer Engineering, North Carolina State University, Raleigh, NC 27695-7911, USA*
*Email: hzhang@ncsu.edu*

**Huaiyu Dai**
*Department of Electrical and Computer Engineering, North Carolina State University, Raleigh, NC 27695-7911, USA*
*Email: Huaiyu_Dai@ncsu.edu*

*Received 1 December 2003; Revised 12 July 2004*

Recently, the remarkable capacity potential of multiple-input multiple-output (MIMO) wireless communication systems was unveiled. The predicted enormous capacity gain of MIMO is nonetheless significantly limited by cochannel interference (CCI) in realistic cellular environments. The previously proposed advanced receiver technique improves the system performance at the cost of increased receiver complexity, and the achieved system capacity is still significantly away from the interference-free capacity upper bound, especially in environments with strong CCI. In this paper, base station cooperative processing is explored to address the CCI mitigation problem in downlink multicell multiuser MIMO networks, and is shown to dramatically increase the capacity with strong CCI. Both information-theoretic dirty paper coding approach and several more practical joint transmission schemes are studied with pooled and practical per-base power constraints, respectively. Besides the CCI mitigation potential, other advantages of cooperative processing including the power gain, channel rank/conditioning advantage, and macrodiversity protection are also addressed. The potential of our proposed joint transmission schemes is verified with both heuristic and realistic cellular MIMO settings.

**Keywords and phrases:** base station cooperation, cochannel interference, dirty paper coding, macrodiversity, rank deficiency, vector broadcast channel.

## 1. INTRODUCTION

In the past few years, demand for broadband wireless data access has grown exponentially. For example, existing third-generation networks provide up to 2 Mbps indoors and 144 kbps in vehicular environments; while the minimum speed currently targeted for fourth-generation systems is 10–20 Mbps indoors and 2 Mbps in moving vehicles. Recently, the remarkable capacity potential of multiple-input multiple-output (MIMO) systems has been unveiled [1, 2]. A (flat-fading) MIMO channel, typically modeled as a matrix with independent and identically distributed (i.i.d.) complex Gaussian entries, provides multiple spatial dimensions for communications and yields a spatial multiplexing gain. At high signal-to-noise ratio (SNR), Shannon capacity can increase linearly with the minimum number of transmit and receive antennas.

However, achieving the predicted enormous capacity gains in realistic cellular multiuser MIMO networks could be problematic. First, for realistic cellular systems, the sharing of common system resources by multiple users and the frequency reuse among adjacent cells will bring in cochannel interference (CCI), which may greatly diminish the advantages of MIMO systems [3]. Another problem in achieving these dramatic capacity gains in practice, especially for outdoor deployment, is the rank deficiency and ill-condition of the MIMO channel matrix. This is mainly caused by the spatial correlation due to insufficient scattering and antenna spacing [4, 5], and sometimes by the "keyhole" effect even though the fading is essentially uncorrelated on each end of the channel [6]. Finally, the effect of the large-scale fading, largely neglected in current MIMO study, may also induce negative impact on the anticipated performance.

The study on the performance of interference-limited multicell multiuser MIMO attracted research attention only recently [3, 7]. The study in [3] indicated the ineffectiveness of a MIMO system in an interference-limited environment, when CCI is treated as background noise. Motivated

by this study, multiuser detection (MUD) and turbo decoding have been explored to significantly improve the performance of MIMO systems in a multicell structure [8, 9]. Such advanced receiver techniques improve the system performance at the cost of increased receiver complexity. While they are readily applicable today at base stations (BSs) or access points (APs) for uplink processing of wireless networks, they still impose challenges for the design of mobile stations (MSs) in downlink communications, which is considered to be the bottleneck for next-generation high-speed wireless systems. Furthermore, it is also found that there is a significant performance gap between the obtained MUD capacity and the single-cell interference-free capacity upper bound, especially in environments with strong CCI. This advocates a need to devote more system resources for performance enhancement in the downlink multicell multiuser MIMO networks.

The idea naturally arises to move the CCI mitigation to the transmitter (BS) side on the downlink, where complex structure and advanced processing can be more easily accommodated, if channel state information (CSI) can be obtained at the transmitter side either through uplink estimation or through a feedback channel, for low user mobility scenarios such as indoor or outdoor pedestrian environments. Moreover, as multiple users in multiple cells are involved, cooperative processing at relevant BSs can be exploited. This approach is feasible, as in the current infrastructure that is common to both cellular communications and indoor wireless internet access, the BSs and APs in the system are connected by a high-speed wired backbone that allows information to be reliably exchanged among them. This approach is also reasonable, as in environments with strong interference, a mobile usually experiences several *comparable* and *weak* links from surrounding radio ports, where soft handoff typically takes place in current CDMA networks. In this scenario, cooperative processing among relevant ports transforms the obstructive interference into constructive signals, which should offer large performance improvement. Joint transmitter preprocessing for single-cell multiuser MIMO communications has aroused much research interest recently (see, e.g., [10, 11, 12]). BS cooperation approach is proposed in [13] to enhance the downlink sum capacity (throughput) with single-input single-output (SISO) systems employed in each cell, by implementing dirty paper coding (DPC) proposed in [14]. In this paper, both information-theoretic DPC and some more practical joint transmission schemes will be studied with cooperative multicell BSs for downlink multiuser MIMO communications. Our analysis in general provides an upper bound for achievable performance with BS cooperation, which defines a common benchmark to gauge the efficiency of any practical scheme. The key contributions of this paper are summarized as follows.

(i) A common framework is proposed for the study of joint transmissions with cooperative BSs for downlink multicell multiuser MIMO networks with both pooled and individual power constraints.

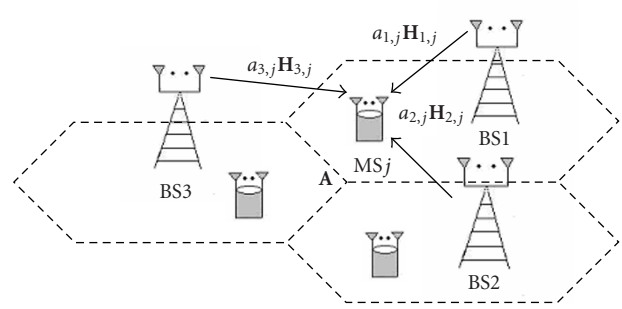


Figure 1: A multicell multiuser MIMO system with $N_b = 3$, $K = 3$.

(ii) The potential of BS cooperative processing on CCI mitigation is explored from both information-theoretic and practical signal-processing standpoints, and is shown to significantly outperform the advanced receiver techniques and conventional noncooperative signaling.

(iii) Other advantages of BS cooperative processing are also addressed, including power gain, channel rank/conditioning advantage, and macrodiversity protection.

(iv) Simulations results with both heuristic and realistic scenarios have been provided to demonstrate these advantages, and some practical concerns including synchronization issues are carefully addressed.

The rest of the paper is organized as follows. The system model and problem formulations are given in Section 2. The concept of BS cooperation together with theoretical and practical joint transmission schemes is discussed in Section 3. Other advantages of BS cooperation including power gain, rank/conditioning advantage, and macrodiversity protection are further addressed in Section 4. Some practical concerns are discussed in Section 5 and numerical results are provided in Section 6 to verify the main points of this paper. Finally, Section 7 contains some concluding remarks.

## 2. SYSTEM MODEL AND PROBLEM FORMULATIONS

Suppose in general that there are $K$ cochannel mobile users arbitrarily distributed in the downlink multicell system, with $N_r$ being the number of receive antennas at each MS, and $N_t$ the number of transmit antennas at each BS, respectively. Suppose that $N_b$ is the total number of cochannel adjacent BSs in the system; so $(N_t, N_r, N_b, K)$ can be used to represent the overall system, as in Figure 1 for a case with $N_b = K = 3$. With nondispersive flat-fading assumption, let $\{\mathbf{H}_{b,j}\}_{b=1}^{N_b}{}_{j=1}^{K}$ be the small-scale fading channel matrix from BS $b$ to MS $j$ with zero-mean unit-variance complex Gaussian entries (assuming rich scattering); and let $\{a_{b,j}\}$ be the corresponding large-scale fading coefficients with $a_{b,j}^2 = \mathrm{PL}_{b,j} S_{b,j}$, where $\mathrm{PL}_{b,j} = \beta_0 d_{b,j}^{-\gamma}$ represents the path loss, with $\beta_0$ a propagation constant, $d_{b,j}$ the propagation

distance, $\gamma$ the path loss exponent, while $S_{b,j}$ denotes the shadow fading, typically modeled as a log-normal random variable with standard deviation $\sigma$. Note that on the downlink, if MS $j$ is in cell $b$, $a_{b,j}\mathbf{H}_{b,j}$ represents an in-cell channel; otherwise, it is an intercell channel.

### 2.1. Traditional noncooperative scenario with single-cell signaling

In this scenario, a mobile only communicates with its own BS, while a BS may accommodate multiple mobile users. A single-user matched filter front-end is implemented at the mobile receiver to convert the received waveform into a discrete-time signal [15]. Let $b_j$ ($b_j \in \{1,\ldots,N_b\}$) represent the associated BS of user $j$. The equivalent discrete-time received signal of user $j$ after matched filtering and sampling can then be expressed as

$$\mathbf{y}_j = a_{b_j,j}\mathbf{H}_{b_j,j}\mathbf{x}_j + \sum_{k\neq j} a_{b_k,j}\mathbf{H}_{b_k,j}\mathbf{x}'_{k\_j} + \mathbf{n}_j, \quad j = 1,2,\ldots,K, \tag{1}$$

where $\mathbf{x}_j$ is the transmitted signal intended for user $j$, and $\mathbf{n}_j$ is the background noise. In (1), the interference signal $a_{b_k,j}\mathbf{H}_{b_k,j}\mathbf{x}'_{k\_j}$ can come from any BS including $b_j$ (when $b_k = b_j$). We assume that the matched filter at MS $j$ can synchronize with the signature waveform of its desired signal, but not with the waveforms of the signals intended for other users. So we use $\mathbf{x}'_{k\_j}$ to represent the equivalent discrete-time transmitted signal intended for user $k$ and asynchronously received at MS $j$ after matched filtering, which is a certain linear combination of two temporally consecutive symbols of $\mathbf{x}_k$. The background noise is assumed to be circularly symmetric complex Gaussian with covariance matrix $\mathbf{\Phi}_n = N_0\mathbf{I}$, where $\mathbf{I}$ denotes an identity matrix. Transmit signals for all $K$ users are assumed to be mutually uncorrelated, and independent of the background noise. In general, a preprocessing $N_t \times L_j$ matrix $\mathbf{T}_j$ is applied to the transmitted data for user $j$ as $\mathbf{x}_j = \mathbf{T}_j\mathbf{s}_j$, where the $L_j \times 1$ vector $\mathbf{s}_j$ represents the actual data intended for user $j$, assumed to have i.i.d. complex Gaussian entries with zero mean and unit variance ($E(\mathbf{s}_j\mathbf{s}_j^H) = \mathbf{I}$). The signal intended for user $j$ is transmitted with a power of $E[\mathrm{Tr}(\mathbf{x}_j\mathbf{x}_j^H)] = \mathrm{Tr}(\mathbf{T}_j\mathbf{T}_j^H) = P_{U\_j}$. If there is no CSI available at the transmitter, the power is equally allocated among $N_t$ transmit antennas at each BS with

$$\mathbf{T}_j = \sqrt{\frac{P_{U\_j}}{N_t}}\mathbf{I}. \tag{2}$$

Otherwise, the transmitter precoding at each BS can be designed as

$$\mathbf{T}_j = \mathbf{V}_j\mathbf{\Lambda}_j, \tag{3}$$

where $\mathbf{V}_j$ collects the first $L_j$ right singular vectors of the desired channel matrix $a_{b_j,j}\mathbf{H}_{b_j,j}$, and $\mathbf{\Lambda}_j$ is a diagonal matrix representing the powers allocated for each eigenmode of user $j$ with the power constraint $P_{U\_j}$. To maximize the mutual information for user $j$, the water-filling algorithm can be used for power allocation. However, it is easy to show that equal power allocation among the $L_j$ nonzero eigenmodes of $a_{b_j,j}\mathbf{H}_{b_j,j}$ will result in a negligible capacity loss compared to water filling, especially at high SNR regime. Therefore, the following transmit signaling is often employed for simplicity:[1]

$$\mathbf{T}_j = \mathbf{V}_j\sqrt{\frac{P_{U\_j}}{L_j}}\mathbf{I}. \tag{4}$$

A lower bound for single-cell signaling schemes can be derived with the conventional single-user detector, which simply treats CCI as an additive white Gaussian noise. The spectral efficiency for user $j$ with this conventional single-user detector is then given by [8]

$$R_{j\_\mathrm{conv}} = \log\left|\mathbf{I} + \frac{a_{b_j,j}^2}{\left(N_0 + \sum_{k\neq j} P_{U\_k}a_{b_k,j}^2\right)}\mathbf{H}_{b_j,j}\mathbf{T}_j\mathbf{T}_j^H\mathbf{H}_{b_j,j}^H\right|, \tag{5}$$

in which $\mathbf{T}_j$ can be designed using (2)–(4) based on the availability of CSI at the transmitter. On the other hand, the single-cell signaling interference-free upper bound unrealistically assumes no interference at the receiver of MS $j$:

$$\begin{aligned} R_{j\_\mathrm{single\ cell}} &= \log\left|\mathbf{I} + \frac{a_{b_j,j}^2}{N_0}\mathbf{H}_{b_j,j}\mathbf{T}_j\mathbf{T}_j^H\mathbf{H}_{b_j,j}^H\right| \\ &= \sum_{l=1}^{L_j}\log\left(1 + \frac{P_l}{N_0}\lambda_l^2\right), \end{aligned} \tag{6}$$

where the second equality follows from the singular value decomposition (SVD) of $a_{b_j,j}\mathbf{H}_{b_j,j}$.

The receiver MUD schemes proposed in [8, 9], including the group linear minimum mean square error (MMSE) detector, the group MMSE successive interference cancellation (SIC) detector, and the adaptive multiuser detector, can improve the performance of MIMO systems in a multicell structure. However, they require MS $j$ to know not only its desired channel, but also the interfering channels, and some receivers may need to detect both the desired and interfering signals. They can be readily implemented at BS for CCI mitigation on the uplink, but may still be impractical for current MS on the downlink because of their complexity. Furthermore, it is found in [8, 9] that the performances of the multiuser receivers are still far from the interference-free upper bound (6), especially in environments with strong interference, which indicates a need to exploit more system resources for throughput enhancement.

[1] Note that signaling (4) is equivalent to (2) for full-rank channels, but significantly different otherwise.

### 2.2. BS cooperation scenario

For BS cooperation schemes, the transmit signal for each user is spread over all $N_b$ BS. Then $\mathbf{x}_j = [\mathbf{x}_j^{[1]T}, \mathbf{x}_j^{[2]T}, \ldots, \mathbf{x}_j^{[N_b]T}]^T$, where $\mathbf{x}_j^{[b]}$ is the transmitted signal intended for user $j$ from BS $b$. With the assumption that the transmitter knows the propagation delay for each BS-MS pair, $\mathbf{x}_j$ can be precompensated for the different delays from different BSs to MS $j$. So MS $j$ can still receive a synchronized $\mathbf{x}_j$:

$$\mathbf{y}_j = \mathbf{H}_{Ej}\mathbf{x}_j + \sum_{k\neq j} \mathbf{H}_{Ej}\mathbf{x}'_{k\_j} + \mathbf{n}_j, \tag{7}$$

where

$$\mathbf{H}_{Ej} = \left[a_{1,j}\mathbf{H}_{1,j}, a_{2,j}\mathbf{H}_{2,j}, \ldots, a_{N_b,j}\mathbf{H}_{N_b,j}\right]_{N_r\times N_t N_b}, \tag{8}$$

and in $\mathbf{x}'_{k\_j} = [\mathbf{x}_{k\_j}^{[1]'T}, \mathbf{x}_{k\_j}^{[2]'T}, \ldots, \mathbf{x}_{k\_j}^{[N_b]'T}]^T$, $\mathbf{x}_{k\_j}^{[b]'}$ represents asynchronous reception of $\mathbf{x}_k^{[b]}$ at MS $j$, given that $\mathbf{x}_k$ cannot be precompensated for MS $j$ during joint transmission. In this scenario, the transmit matrices $\{\mathbf{T}_j\}$ are of the dimension $N_t N_b \times L_j$, and $\{\mathbf{T}_j\}_{j=1}^K$ are designed only based on the characteristics of $\{\mathbf{H}_{Ej}\}_{j=1}^K$, which are assumed to be constant over a much longer period than the largest delay among all BS-MS pairs in the system, with the quasistatic fading channel assumption. So $\{\mathbf{T}_j\}$ are constant during this time period and we have $\mathbf{x}'_{k\_j} = \mathbf{T}_k\mathbf{s}'_{k\_j}$, where $\mathbf{s}'_{k\_j} = [\mathbf{s}_{k\_j}^{[1]'T}, \mathbf{s}_{k\_j}^{[2]'T}, \ldots, \mathbf{s}_{k\_j}^{[N_b]'T}]^T$, and $\mathbf{s}_{k\_j}^{[b]'}$ is the corresponding asynchronous reception of the substreams in $\mathbf{s}_k$ transmitted from BS $b$, as discussed above. Therefore, (7) can be rewritten as

$$\mathbf{y}_j = \mathbf{H}_{Ej}\mathbf{T}\mathbf{s}_{[j]} + \mathbf{n}_j, \tag{9}$$

where $\mathbf{T} = [\mathbf{T}_1, \mathbf{T}_2, \ldots, \mathbf{T}_K]_{N_t N_b \times \sum_k L_k}$, and $\mathbf{s}_{[j]}^T = [\mathbf{s}'^T_{1\_j}, \ldots, \mathbf{s}'^T_{j-1\_j}, \mathbf{s}_j^T, \mathbf{s}'^T_{j+1\_j}, \ldots, \mathbf{s}'^T_{K\_j}]_{\sum_k L_k \times 1}$. For simplicity, we still assume that $\{\mathbf{s}'_{k\_j}\}$ have i.i.d. complex Gaussian entries with zero mean and unit variance.

The key problem of joint transmit processing among cooperative BSs is to jointly design a transmit matrix $\mathbf{T}$ to mitigate CCI and enhance the system spectral efficiency with either a pooled power constraint

$$E\left[\sum_{k=1}^K \mathrm{Tr}\left(\mathbf{x}_k\mathbf{x}_k^H\right)\right] = \mathrm{Tr}\left(\sum_{k=1}^K \mathbf{T}_k\mathbf{T}_k^H\right) \le P_t, \tag{10}$$

or more practical per-base power constraints

$$\begin{aligned} E\left[\sum_{k=1}^K \mathrm{Tr}\left(\mathbf{x}_k^{[b]}\mathbf{x}_k^{[b]H}\right)\right] &= \mathrm{Tr}\left(\mathbf{T}^{[b]}\mathbf{T}^{[b]H}\right) \\ &= \mathrm{Tr}\left(\sum_{k=1}^K \mathbf{T}_k^{[b]}\mathbf{T}_k^{[b]H}\right) \\ &\le P_{B\_b}, \quad b = 1, 2, \ldots, N_b, \end{aligned} \tag{11}$$

where $\mathbf{T}^{[b]}$ and $\mathbf{T}_k^{[b]}$ are the rows in $\mathbf{T}$ and $\mathbf{T}_k$ corresponding to the transmit antennas at BS $b$, respectively. In our study, since MS $j$ is not interested in correctly detecting $\mathbf{s}_k$, for $k \neq j$, the design of the joint transmit matrix $\mathbf{T}$ is actually not affected by the asynchronous receptions of interfering signals and $\{\mathbf{s}'_{k\_j}\}$ can be simply viewed as the data of some virtual synchronous interfering users.

## 3. JOINT TRANSMISSION TECHNIQUES WITH BASE STATION COOPERATION

As seen in Figure 1, by cooperating the $N_b$ adjacent BSs, the downlink of a $(N_t, N_r, N_b, K)$ multicell multiuser MIMO system forms a vector broadcast channel (BC), in which the $NT = N_t \times N_b$ transmit antennas are distributed among the $N_b$ radio ports (or BSs). Unlike traditional BC with colocated MIMO channels, the channel gains from any two antenna elements at different BSs are independent. With BS cooperation, the system resources can be pooled together for more efficient use. In particular, the severe CCI problem can be effectively controlled and significant performance improvement can be achieved. Meanwhile, the complexity at MS can be significantly reduced.

In the following, the potential of cooperative processing for system capacity enhancement is first studied from a theoretical standpoint, by extending the DPC approach with a pooled power constraint (10) to the downlink multicell multiuser scenario. Then some more practical suboptimal transmission schemes with more practical per-base power constraints (11) will also be investigated.

### 3.1. Performance upper bound: dirty paper coding with pooled power constraint

For a system with perfect data and power cooperation among $N_b$ BSs, we can implement the throughput-achieving DPC [2, 14], at the vector BC formed by cooperative BSs, to obtain a system performance upper bound. Note that with the asynchronous vector BC model (7), we apply DPC in a slightly different way, where the encoder for the "current" user needs to noncausally know not only the encoding of "previous" users and associated CSI, but also the corresponding propagation delays to precancel the interference from "previous" users. The rate of each user and the (optimal) sum rate can then be expressed as

$$R_{\pi(j)\_\mathrm{DPC}}(\mathbf{T}) = \log \frac{\left|N_0\mathbf{I} + \mathbf{H}_{E\pi(j)}\left(\sum_{k\ge j}\mathbf{T}_{\pi(k)}\mathbf{T}_{\pi(k)}^H\right)\mathbf{H}_{E\pi(j)}^H\right|}{\left|N_0\mathbf{I} + \mathbf{H}_{E\pi(j)}\left(\sum_{k>j}\mathbf{T}_{\pi(k)}\mathbf{T}_{\pi(k)}^H\right)\mathbf{H}_{E\pi(j)}^H\right|}, \tag{12}$$

$$\mathrm{SR}_{\mathrm{DPC}} = \max_{\mathrm{Tr}(\mathbf{T}\mathbf{T}^H)=P_t,\pi}\left(\sum_{\pi(j)} R_{\pi(j)\_\mathrm{DPC}}(\mathbf{T})\right), \tag{13}$$

where $\mathbf{T}$ is given in (9), and $\pi(1), \pi(2), \ldots, \pi(K)$ represents a certain user ordering. By applying the duality of the BC and multiple-access channel (MAC) [16], (13) can be obtained by calculating the sum rate of a dual MAC with the same total power constraint $P_t$. Iterative numerical methods that

jointly optimize (13) on the dual uplink were proposed (see, e.g., [17, 18]) based on the iterative water-filling algorithm proposed in [19]. Furthermore, it is shown that (13) is actually the saddle point (with worst-case colored noise) of the Sato's bound, which is the sum rate of a heuristic cooperative system where both transmitters and receivers can cooperate with each other, given by [20]

$$\mathrm{SR}_{\mathrm{Sato}} = \max_{\mathrm{Tr}(\mathbf{T}\mathbf{T}^H)\le P_t} \log \frac{\left|\mathbf{\Phi}_n + \mathbf{H}_T\mathbf{T}\mathbf{T}^H\mathbf{H}_T^H\right|}{\left|\mathbf{\Phi}_n\right|}, \tag{14}$$

where $\mathbf{H}_T = [\mathbf{H}_{E1}^T, \mathbf{H}_{E2}^T, \ldots, \mathbf{H}_{EK}^T]^T$ and $\mathbf{\Phi}_n$ is the noise covariance matrix.

In [13], the concept of DPC on cooperative BS is proposed with a simple scalar channel for each cell. A suboptimal algorithm, DPC with linear preprocessing (LP-DP), is exploited to simplify the optimization procedure involved in (13), with a negligible performance penalty. It is also proved that LP-DP is asymptotically optimal at high SNR [21]. For the special case of $K = N_b$, we can extend LP-DP to our multicell MIMO vector BC scenario as in Appendix A. In short, by applying LQ decompositions and DPC, we can get $K$ parallel interference-free channels for the $K$ users, with the sum rate

$$\mathrm{SR}_{\text{LP-DP}} = \sum_{j=1}^{K}\sum_{l=1}^{L_j} \log\left|1 + \frac{P_{j,l}\lambda_{j,l}^2}{N_0}\right|, \tag{15}$$

where $P_{j,l}$ and $\lambda_{j,l}$ are the allocated power and singular value for the $l$th nonzero eigenmode of user $k$'s virtual interference-free channel, respectively.

DPC with per-base constraints is much more involved, as the MAC/BC duality does not hold any more. DPC has not been shown to achieve the capacity region or even the sum capacity with constraints (11). Complex iterative multistage numerical methods for cooperative DPC with constraints (11) are proposed in [2, 22, 23], in which a small piece of power is invested to a certain selected user until one of the BS reaches its power constraint. The path gains corresponding to this BS are then set to zero in subsequent stages so that no further power is allocated to these antennas. In general, (11) is more strict than (10), so a performance degradation is expected.

Although the DPC scheme with a pooled power constraint gives us a simple performance upper bound for BS cooperation, some unrealistic assumptions are made, such as the noncausal knowledge of interference sequence at the transmitter, which motivates the exploration of more practical joint transmission schemes, as will be discussed in the following.

### 3.2. Suboptimal joint transmission schemes for BS cooperation with per-base power constraints

DPC is an information theoretical approach that can demonstrate the potential of joint transmission with cooperative processing. In this part, several suboptimal but more practical joint transmission schemes with the more practical per-base power constraints are exploited for better understanding of the achievable performance gains of BS cooperative processing in practice. Essentially these techniques are counterparts of corresponding multiuser detectors, some of which have been revisited in the colocated MIMO context recently [10, 24, 25]. These suboptimal joint transmission schemes will be compared with both the receiver MUD approaches [8, 9] and DPC approaches in Section 6.1. In general, the following expression holds true for the spectral efficiencies of user $j$ with these joint linear transmission schemes (except TDMA):

$$R_{j\_\text{subopt}}(\mathbf{T}) = \log\left|\mathbf{I} + \left[N_0\mathbf{I} + \mathbf{H}_{Ej}\left(\sum_{i\ne j}\mathbf{T}_i\mathbf{T}_i^H\right)\mathbf{H}_{Ej}^H\right]^{-1}\mathbf{H}_{Ej}\mathbf{T}_j\mathbf{T}_j^H\mathbf{H}_{Ej}^H\right|, \tag{16}$$

where different schemes correspond to different choices of transmission matrices $\{\mathbf{T}_j\}$ or $\mathbf{T}$ with the constraints (11). As discussed in Section 2, the design of $\{\mathbf{T}_j\}$ only depends on $\{\mathbf{H}_{Ej}\}$, but not on the transmitted signals, so the asynchronous receptions in (7) assume no influence on such designs, if precompensation for each user's data is implemented at the joint transmitter. Intuitively, compared with DPC, (16) may induce more transmit power inefficiency, as $\mathbf{T}$ is responsible for the mitigation of interference from both "previous" and "subsequent" users, and per-base power constraints are implemented instead of a pooled power constraint.

Before discussing these suboptimal joint transmission schemes in detail, we first propose a simple algorithm for designing $\mathbf{T}$ with per-base power constraints. Let $L_T = \sum_{k=1}^{K} L_k$ be the overall number of data streams of $K$ users. Suppose that a preliminary joint linear transmit matrix $\mathbf{G}_{N_bN_t\times L_T}$ is given, whose designs will be introduced in the sequel. Our design of $\mathbf{T}$ with per-base power constraints (11) is given by

$$\mathbf{T} = \mathbf{G}\cdot\mathbf{\Omega}, \tag{17}$$

where $\mathbf{\Omega}$ is an $L_T\times L_T$ diagonal matrix with diagonals $\{\mu_l\}_{l=1}^{L_T}$, each representing the allocated power for the corresponding original data stream. Since typically $L_T \gg N_b$ and there are only $N_b$ per-base power constraints in (11), we can further divide $\{\mu_l\}_{l=1}^{L_T}$ into $N_b$ groups, each with $L_T/N_b$ elements having the same value:

$$\mathbf{\Omega} = \mathrm{blockdiag}\left(\mu_1\mathbf{I}, \mu_2\mathbf{I}, \ldots, \mu_{N_b}\mathbf{I}\right). \tag{18}$$

Further define

$$\mathbf{Q}_{N_b\times N_b} = \begin{bmatrix} \left\|\mathbf{G}_1^{[1]}\right\|_F^2 & \left\|\mathbf{G}_2^{[1]}\right\|_F^2 & \cdots & \left\|\mathbf{G}_{N_b}^{[1]}\right\|_F^2 \\ \left\|\mathbf{G}_1^{[2]}\right\|_F^2 & \left\|\mathbf{G}_2^{[2]}\right\|_F^2 & \cdots & \left\|\mathbf{G}_{N_b}^{[2]}\right\|_F^2 \\ \vdots & \vdots & \vdots & \vdots \\ \left\|\mathbf{G}_1^{[N_b]}\right\|_F^2 & \left\|\mathbf{G}_2^{[N_b]}\right\|_F^2 & \cdots & \left\|\mathbf{G}_{N_b}^{[N_b]}\right\|_F^2 \end{bmatrix}, \tag{19}$$

where $\mathbf{G}_j^{[b]}$ is an $N_t \times L_T/N_b$ submatrix in $\mathbf{G}$, corresponding to the transmit weights at BS $b$ for the $j$th group of data streams as defined above. Let $\mathbf{P} = [P_{B\_1}, P_{B\_2}, \ldots, P_{B\_N_b}]^T$ be the per-base power constraint vector. Then we can calculate $\boldsymbol{\Omega}$ by solving the linear system equation

$$\boldsymbol{\mu} = [\mu_1^2, \mu_2^2, \ldots, \mu_{N_b}^2]^T = \mathbf{Q}^{-1}\mathbf{P}. \tag{20}$$

When an infeasible solution ($\boldsymbol{\mu}$ does not have all positive entries) is obtained, we can refine it as

$$\boldsymbol{\Omega} = \mu\mathbf{I}, \quad \mu = \min_{b=1,2,\ldots,N_b}\left(\frac{P_{B\_b}}{||\mathbf{G}^{[b]}||_F^2}\right), \tag{21}$$

where $\mathbf{G}^{[b]}$ is the rows of $\mathbf{G}$ corresponding to transmit antennas at BS $b$. Note that (20) can utilize the full power at each BS, while in (21), only the BS satisfying the minimum value can transmit with full power and any other BS transmits with a power less than its power constraint. Nonetheless, it has been shown that designs with per-base power constraints incur insignificant performance loss for linear joint transmission schemes compared to the corresponding designs with pooled power constraint, thus demonstrating the applicability of these joint transmission schemes in realistic cellular communications. These suboptimal schemes are illustrated as follows.

#### TDMA

The simplest way of totally eliminating CCI is to implement time-division multiple access (TDMA) in the multicell downlink. At each time slot, the network services one single user, and all the antenna elements and transmit power are employed for such transmission, with the precompensation of different delays. The spectral efficiency of user $j$ with joint TDMA signaling is then given by

$$R_{j\_\,\mathrm{TDMA}} = \frac{1}{K}\log\left|\mathbf{I} + \mathbf{H}_{Ej}\mathbf{T}\mathbf{T}^H\mathbf{H}_{Ej}^H\right|, \tag{22}$$

with the joint transmission matrix $\mathbf{T} = \mathbf{G}\cdot\boldsymbol{\Omega}$ exclusively designed for user $j$. During the time slot for user $j$, the preliminary transmission matrix can be expressed by $\mathbf{G} = [\mathbf{0}, \mathbf{0}, \ldots, \mathbf{V}_j, \ldots, \mathbf{0}]$, in which $\mathbf{V}_j$ collects the first $L_j$ right singular vectors of $\mathbf{H}_{Ej}$. Since (19) is singular, the diagonal matrix $\boldsymbol{\Omega}$ is calculated by (21) to satisfy the per-base power constraint as discussed above. As is already known, from the system capacity viewpoint, it is beneficial to serve multiple users simultaneously and actively control the CCI rather than to allow one single user to occupy the whole system resource exclusively. This is also verified from our numerical results in Section 6.1.

#### Single-user eigenbeamforming

This approach can be viewed as the counterpart of the conventional single-user detector (see (5)), which implements eigenbeamforming for each user with respect to the corresponding channel matrix without considering the CCI. Thus we have $\mathbf{G}_j = \mathbf{V}_j$, where $\mathbf{V}_j$ is defined as in the TDMA scheme, and $\mathbf{G} = [\mathbf{G}_1, \mathbf{G}_2, \ldots, \mathbf{G}_K]$. Compared with single-cell signaling systems, this scheme only achieves a power gain, which will be introduced in Section 4.1.

#### JT-ZF

Joint transmitter zero forcing (JT-ZF) approach can be viewed as the counterpart of the multiuser decorrelator, which employs a pseudoinverse of $\mathbf{H}_T = [\mathbf{H}_{E1}^T, \mathbf{H}_{E2}^T, \ldots, \mathbf{H}_{EK}^T]^T$ with

$$\mathbf{G} = \mathbf{H}_T^H\left(\mathbf{H}_T\mathbf{H}_T^H\right)^{-1}, \qquad \mathbf{T}_j = \mathbf{G}_j\cdot\boldsymbol{\Omega}_j, \tag{23}$$

where $\boldsymbol{\Omega}_j$ is the corresponding $j$th $L_j \times L_j$ diagonal block of $\boldsymbol{\Omega}$. With this approach, we can easily get

$$\mathbf{H}_{Ej}\cdot\mathbf{T}_i = \begin{cases}\boldsymbol{\Omega}_i\mathbf{I}, & i = j,\\ \mathbf{0}, & i \neq j.\end{cases} \tag{24}$$

Then (7) can be rewritten as $\mathbf{y}_j = \boldsymbol{\Omega}_j\mathbf{s}_j + \mathbf{n}_j$, and interference from both other users and other substreams of the same user are eliminated simultaneously. Just as ZF receivers eliminate the interference at the expense of noise enhancement, ZF transmitters generally increase the average transmit power by the same factor. Furthermore, in the rank deficient scenario where $\mathbf{H}_T\mathbf{H}_T^H$ is singular, this approach cannot even be applied. These observations naturally motivate the joint transmission design based on MMSE criterion.

#### JT-MMSE

Recalling the tradeoff between interference cancellation and noise enhancement for its receiver counterpart, joint transmitter MMSE (JT-MMSE) makes a good tradeoff between interference cancellation and transmitter power efficiency, whose preliminary joint transmission matrix is given as

$$\mathbf{G} = \mathbf{H}_T^H\left(\mathbf{H}_T\mathbf{H}_T^H + \frac{N_0}{P_t}\mathbf{I}\right)^{-1}. \tag{25}$$

#### JT-decomp

For this approach, the preliminary transmission matrix for user $j$ can be described as

$$\mathbf{G}_j = \overline{\mathbf{V}}_j\mathbf{V}_j', \tag{26}$$

where $\overline{\mathbf{V}}_j$ includes the right singular vectors corresponding to the null space (zero singular values) of $\overline{\mathbf{H}}_{T\_j} = [\mathbf{H}_{E1}^T, \ldots, \mathbf{H}_{Ej-1}^T, \mathbf{H}_{Ej+1}^T, \ldots, \mathbf{H}_{EK}^T]^T$, and $\mathbf{V}_j'$ includes the first $L_j$ right singular vectors of the virtual channel $\mathbf{H}_{Ej}' = \mathbf{H}_{Ej}\overline{\mathbf{V}}_j$. $\overline{\mathbf{H}}_{T\_j}$ usually has a nonzero null space, so $\mathbf{H}_{Ei}\overline{\mathbf{V}}_j = \mathbf{0}$, $i \neq j$, can be guaranteed. Interference from all other users is cancelled, and we obtain a set of equivalent parallel interference-free subchannels $\{\mathbf{H}_{Ej}'\}$.

The joint transmitter null-space decomposition (JT-decomp) approach generally outperforms JT-MMSE and JT-ZF at the cost of extra complexity, as will be seen in our numerical results. There is again a potential problem with this

approach in the rank deficient scenario. If $\mathbf{H}_{Ej}$ is rank deficient, there will be a higher chance that null($\overline{\mathbf{H}}_{T\_j}$) overlaps with null($\mathbf{H}_{Ej}$), which means that the equivalent channel $\mathbf{H}'_{Ej}$ may have reduced channel rank or even null rank (when null($\overline{\mathbf{H}}_{T\_j}$) = null($\mathbf{H}_{Ej}$)). Fortunately, as we will illustrate in the next section, this will rarely happen in our distributed multicell MIMO setting, as compared to the traditional colocated MIMO.

## 4. OTHER ADVANTAGES OF BASE STATION COOPERATION

With BS cooperation, all antennas of the relevant multicell BSs can be jointly employed for data processing and transmission. In some sense, it is equivalent to a single giant BS or processing center. The key differences from the single-cell scenario with colocated antennas at one BS are the widely distributed antennas and independent large-scale fading experienced for each link between a mobile-port pair. Besides its potential in CCI cancellation, BS cooperative processing assumes other advantages in multicell MIMO communications, as indicated below.

### 4.1. Power gain

Considering a single-user interference-free channel with a transmit power constraint $P_{U\_j}$ with BS cooperation, the channel changes from an $N_r \times N_t$ matrix $a_{b_j,j}\mathbf{H}_{b_j,j}$ to an $N_r \times N_t N_b$ matrix $\mathbf{H}_{Ej}$, so we get a channel power gain. Typically $N_t$ is larger than $N_r$ on the downlink, so both matrices have a rank of $N_r$ in rich scattering environment. From the single-user spectral efficiency expression (6), based on the fact that $\sum_i \lambda_i^2 = \|\mathbf{H}\|_F^2$, it is easily seen that with the same channel rank, power constraint, and power allocation algorithm, the higher the channel power, the larger the spectral efficiency. Specifically, the equivalent single-user channel power for single-cell interference-free channel $a_{b_j,j}\mathbf{H}_{b_j,j}$ is given by $a_{b_j,j}^2 E[\|\mathbf{H}_{b_j,j}\|_F^2] = a_{b_j,j}^2 N_t N_r$, while the single-user channel power with BS cooperation is given by $E[\|\mathbf{H}_{Ej}\|_F^2] = (a_{b_j,j}^2 + \sum_{b\neq b_j} a_{b,j}^2)\cdot N_t N_r$. Note that by comparing the above two equations, the relative power gain is significant if MS $j$ has comparable links to adjacent BSs, which represents a strong CCI case. It will typically result in a parallel shift of the spectral efficiency versus SNR curve at high SNR.

In general, for joint transmission schemes, transmit matrix $\mathbf{T}$ uses a portion of the total power for interference mitigation, and the per-base power constraint (11) may also reduce the available power. Such transmit power inefficiency may compromise the power gain achieved by BS cooperation. This effect is sometimes eminent for suboptimal linear joint transmission schemes in Section 3.2, as will be shown in the numerical results of Section 6.1.

### 4.2. Channel rank and conditioning advantages

The capacity of a MIMO system is determined by the characteristics of the channel matrix $\mathbf{H}$. Clearly $r = \text{rank}(\mathbf{H})$ is one such important factor which determines the number of parallel subchannels that can be opened up for independent communications. In rich-scattering environments, full rank can be assumed and essentially $r = \min(N_t, N_r)$ more bps/Hz are obtained for every 3 dB increase in power. However, in some extreme environments (e.g., the keyhole problem [6]), a MIMO system will lose its capacity advantage (spatial multiplexing gain) over a SISO system, even though other advantages like diversity and array gains may still preserve. Another important factor influencing the MIMO capacity is the channel condition number $\kappa = \max_i \lambda_i / \min_i \lambda_i$, or more generally the singular value distribution of the channel matrix. Noting that equal power allocation achieves optimal performance at high SNR in the full channel rank case, we conclude from (6) by Jensen's inequality that a channel with $\kappa = 1$ has the largest capacity, with the same power constraint. In rich scattering environment, channel matrix $\mathbf{H}$ is assumed to have normalized i.i.d. complex Gaussian entries and thus is well-conditioned. In realistic environments, $\mathbf{H}$ may get ill-conditioned due to fading correlation, resulting from the existence of few dominant scatterers, small angle spread, and insufficient antenna spacing [5]. From (6), we see that those subchannels with $\lambda_l^2 \ll 1$ are essentially of no use, even though the channel still has a full rank.

In a typical outdoor urban scenario, antenna arrays at the BSs are elevated above urban clusters and far away from local scattering, while mobile terminals are surrounded by rich scatterers, and the number of independent paths is limited by few far-field reflectors [4]. Therefore, the downlink channel matrix with colocated transmit array can be modeled as

$$\mathbf{H} = c\mathbf{H}_w \mathbf{A}_t^H, \tag{27}$$

where $\mathbf{A}_t$ collects the dominant transmit array response vectors, $\mathbf{H}_w$ is a normalized white Gaussian matrix, and $c$ is the normalization factor. In this case, the channel matrix may be both rank-deficient and ill-conditioned, determined by the propagation and system parameters.

For BS cooperation in multicell MIMO, the overall transmit array is distributed among cooperative BSs, so in the equivalent channel for user $j$ $\mathbf{H}_{Ej} = [a_{1,j}\mathbf{H}_{1,j}, a_{2,j}\mathbf{H}_{2,j}, \ldots, a_{N_b,j}\mathbf{H}_{N_b,j}]$, $\{\mathbf{H}_{b,j}\}_{b=1}^{N_b}$ (all modeled as (27) for outdoor deployment) are independent of each other. The overall number of independent links is then given by $\sum_{b=1}^{N_b} \text{rank}(\mathbf{H}_{b,j})$, which is guaranteed to be at least equal to $N_b$. If $N_b \geq N_r$, $\mathbf{H}_{Ej}$ will always have a full rank. Furthermore, the channel conditioning will not be greatly degraded even if transmit fading correlation happens at each BS, as the fading between different transmit antennas at different BSs is still uncorrelated.

Because of the channel rank and conditioning advantages with BS cooperation, joint transmission schemes in Section 3 will not significantly degrade, compared to single-cell signaling with colocated antennas. In particular, the chance that JT-ZF cannot be implemented, or the chance that null($\overline{\mathbf{H}}_{T\_i}$) overlaps with null($\mathbf{H}_{Ei}$) for JT-decomp (refer to Section 3.2), will be greatly reduced. These suboptimal joint transmission schemes will be shown to even outperform the single-cell upper bound at high SNR for rank deficient channels.

### 4.3. Macrodiversity protection for shadowing channels

Shadowing in wireless channels is a position-sensitive factor, which means that signals from transmit antennas co-located at the same BS are generally subject to the same shadowing, while those from different BSs are subject to independent shadowing. Under severe shadowing, the capacity of a single-cell MIMO with colocated antennas will degrade significantly. On the other hand, cooperative BSs can provide the macrodiversity protection for shadowing impairment because of their independency. Intuitively, the probability that all subchannels of $\mathbf{H}_{Ej}$ are under deep shadow fading is much lower than that of a colocated MIMO channel. Macrodiversity cannot increase the mean of the received SNR, but will greatly reduce its variance. This resulting gain with respect to the outage capacity will be demonstrated in Section 6.3.

## 5. SOME PRACTICAL CONCERNS

Previous studies, such as those in [2, 13, 22, 23], ignored the issues of asynchronous receptions for tractable analysis. In our study, we assume that the cooperative BSs can precompensate different delays in $\mathbf{x}_j$, which results in its synchronous reception at MS $j$, while interfering signals are still received asynchronously. However, for some scenarios involving fast-fading and/or high mobility, the precompensation may require too much system resource. When such joint synchronization among different BSs is not available, we can then either implement more complex signal processing based on asynchronous system models, which directs our future research, or simply restrict our attention to the scenario where cochannel users are all around the cell borders (e.g., around point **A** in Figure 1) where soft-handoff takes place so that the synchronous receptions of both desired and interfering signals can be assumed. To summarize, our analysis in general provides an upper bound for achievable performance with BS cooperation, which defines a common benchmark to gauge the efficiency of any practical schemes. This upper bound becomes rather tight when joint synchronization among different BSs is available through, for example, GPS devices. Clearly the system performance is improved at the cost of significant system overhead related to CSI feedback and information exchange, which should be carefully justified in specific scenarios.

## 6. NUMERICAL RESULTS

In this section, simulation results are presented for both heuristic and practical cellular scenarios to fully demonstrate the potential of BS cooperation processing in downlink multicell multiuser MIMO networks. Sections 6.1–6.3 simulate an ideal symmetric strong CCI scenario, which is similar to the Wyner's model [13, 26], and reveals the achievable performance bounds for BS cooperative processing schemes; meanwhile, Section 6.4 investigates the performance advantage of BS cooperation over traditional single-cell signaling schemes in a realistic cellular scenario.

### 6.1. Performance under Rayleigh fading

A simple *symmetric* three-cell scenario $(2, 2, 3, 3)$ multicell MIMO network with three cochannel users located in three different cells (Figure 1) is considered, which may represent TDMA, FDMA, or orthogonal CDMA. We also assume that $a_{b,j}^2 = 0.5$ (no shadowing), for all $b \neq b_j$, normalized with respect to the in-cell large-scale fading $\{a_{b_j,j}^2\}_{j=1}^3 = 1$, without loss of generality, which represents a strong CCI scenario. For single-cell signaling schemes, data for each user is transmitted with an identical power $\{P_{U\_j}\}_{j=1}^K = P$. Rayleigh fading is assumed. Optimal DPC (13) is obtained through the numerical algorithm in [17], and LP-DP is implemented according to Appendix A. Pooled power constraint is imposed for DPC schemes with $P_t = 3P$, while per-base constraints (11) are enforced for all the other suboptimal BS cooperation schemes. The sum rates of BS cooperation schemes and Sato's bound are divided by three to represent the average rate per user, for a fair comparison with the single-cell signaling schemes. Also, the lower and upper bounds in single-cell approaches, (5) and (6), and the spectral efficiency of the optimal multiuser receiver from [8] are given for reference. The rate curves averaged over all fading states (ergodic rates) are plotted in Figure 2 with respect to average transmit SNR per user, given as $\rho = P/N_0$.

From Figure 2, we see that the performance of the optimal multiuser receiver is still significantly away from the single-cell upper bound. On the other hand, the DPC schemes for BS cooperation result in a significant performance gain over the multiuser receivers, and they even outperform the single-cell upper bound and approach the Sato's upper bound at high SNR. Particularly, the approximate 2 bps/Hz gap between the Sato's bound (as well as DPC schemes) and single-cell upper bound at high SNR, which is resulted from the power gain, can be verified through their equivalent channel power evaluation (see Appendix B).

As discussed in Section 4.1, suboptimal joint transmission schemes reduce interference at the expense of transmitter power inefficiency, which may compromise the power gain and may result in a performance worse than the single-cell interference-free upper bound. This can be observed in Figure 2. Nonetheless, all these suboptimal joint transmission schemes except the single-user eigenbeamforming significantly outperform the multiuser receivers, thus verifying the capability of BS cooperation in practical deployment. Furthermore, from Figure 2, we can see that the JT-decomp approach outperforms JT-MMSE at the cost of extra complexity, and that JT-ZF converges to JT-MMSE at high SNR, which is a well-known result. TDMA performs worse than JT-ZF at high SNR, where JT-ZF's interference cancellation advantage becomes more eminent, which confirms our previous prediction.

It is not difficult to prove that power gain is the major factor influencing the spectral efficiency at low SNR. Therefore, the single-user eigenbeamforming with BS cooperation is better than the receiver MUD at low SNR because of its power gain; but it gets worse at high SNR because it does not actively mitigate the interference. The gap between the

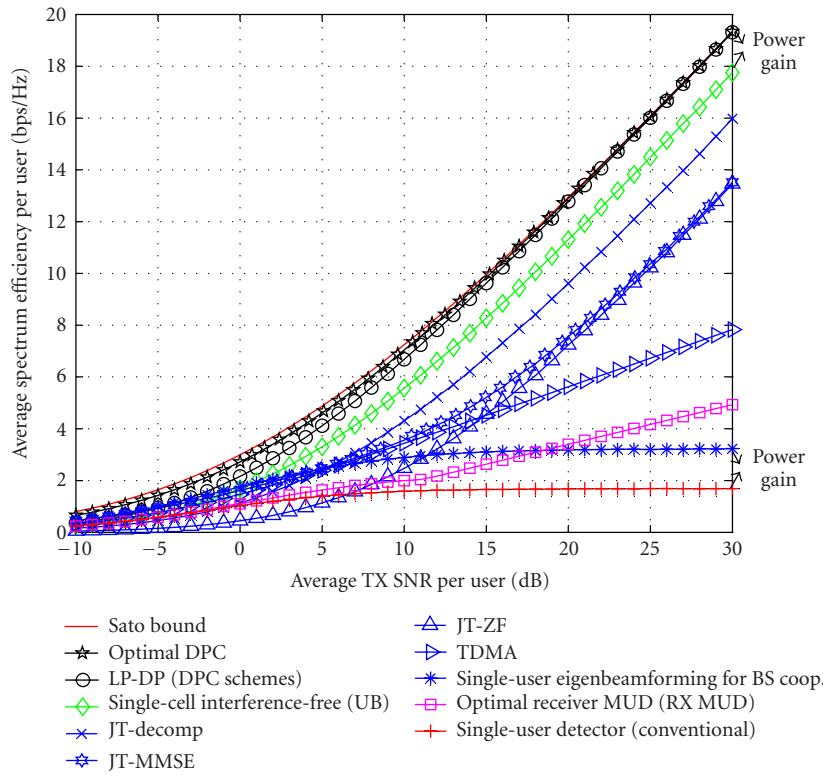


Figure 2: Spectral efficiencies for Rayleigh fading ((2,2,3,3) symmetric scenario).

single-user eigenbeamforming with BS cooperation and the conventional single-user detector is the same as the gap between Sato's bound and single-cell upper bound due to the power gain.

### 6.2. Rank deficient case

Now we use the same parameter setting as in Section 6.1, except that the channel model of (27) is used for $\{\mathbf{H}_{b,j}\}$ with one dominant path, so the ranks of $\{\mathbf{H}_{b,j}\}$ are one. From Figure 3, we can see that the spectral efficiencies of single-cell signaling schemes and the single-cell upper bound degrade (cf. Figure 2) because of the reduced channel rank. Notice that different rank results in different slopes of the rate curves. From Figure 3, we can see that there is a 2 more bps/Hz spectral efficiency gain for every 3 dB transmit SNR increase for BS cooperation schemes, while there is only a 1 bps/Hz gain with the same transmit SNR increase for the single-cell upper bound. That is why JT-ZF and JT-decomp can even outperform the single-cell upper bound at high SNR, as the spatial multiplexing gain compensates the power inefficiency. Thanks to channel rank and conditioning advantages with BS cooperation, performances of all joint transmission schemes do not deteriorate significantly in this deficient channel (cf. Figure 2), including the otherwise problematic JT-ZF and JT-decomp schemes.

### 6.3. Macrodiversity

In this simulation, besides the path loss as defined in Section 6.1, shadowing effect is considered for $\{a_{b,j}\}$ which are independent for different BSs. $p = 10\%$ outage capacity is evaluated for the same $(2, 2, 3, 3)$ symmetric scenario as above. In Figure 4, we compare the outage spectral efficiency of the single-cell interference-free upper bound with that of the BS cooperation scheme JT-decomp (26), with the shadowing standard deviation $\sigma$ ranging from 6 dB to 15 dB. Rayleigh fading is again assumed for $\{\mathbf{H}_{b,j}\}$. Because of the macrodiversity protection, we can see that the outage spectral efficiency of JT-decomp is much more robust than that of the single-cell upper bound when subject to shadow fading outperforming it at severe shadowing scenarios.

### 6.4. Simulation of a realistic cellular scenario

We now further consider a more realistic $(2, 2, 3, 3)$ system in which users with low mobility can be arbitrarily located so that average CCI for each user will be reduced compared with the scenario assumed in Sections 6.1–6.3. Suppose that in a realistic downlink scenario as in Figure 5, three BSs use the same frequency band. By using 120-degree sectoring in each cell, we are interested only in the shadowed area in which three users are uniformly distributed. The radius of each cell is 1000 m, which represents an urban scenario. We only consider the interference from three BSs. Signals from other far away BSs can be approximately treated as additive white Gaussian noise. Rayleigh fading is assumed for small-scale fading. For the large-scale fading $a_{b,j}^2 = \mathrm{PL}_{b,j} S_{b,j}$, an urban-area-based path loss expression $\mathrm{PL}_{b,j} = \beta_0 d_{b,j}^{-\gamma}$ is employed with $\beta_0 \approx 1.35 \times 10^7$ and $\gamma = 3$ [27], while shadow fading $S_{b,j}$ is simulated with $\sigma = 8$ dB.

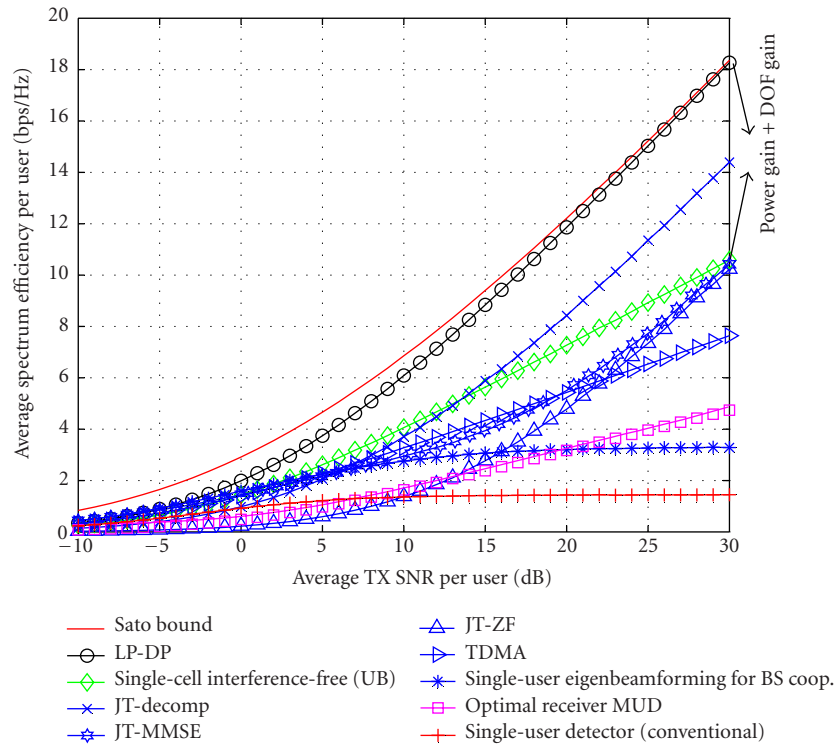


FIGURE 3: Spectral efficiencies for rank deficient subchannels ((2,2,3,3) symmetric scenario).

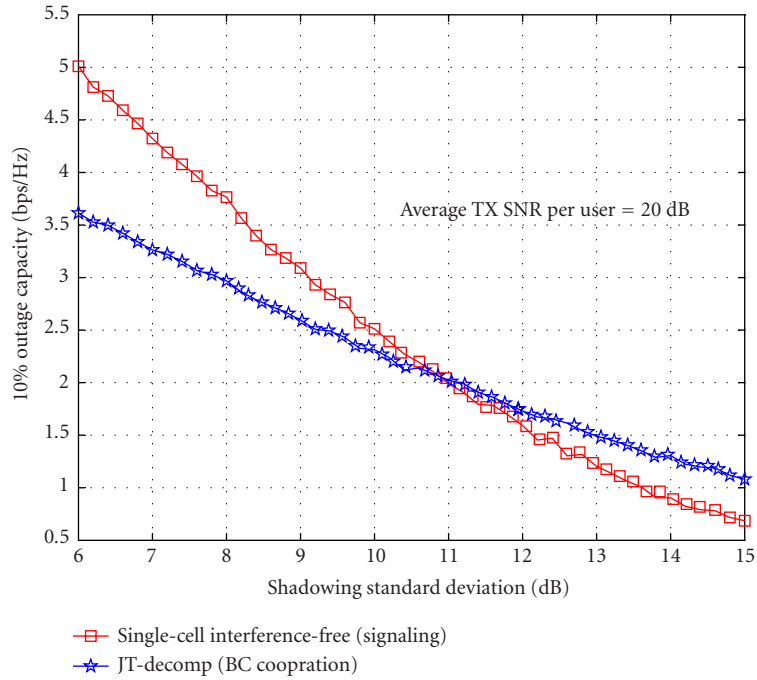


FIGURE 4: Spectral efficiencies for Rayleigh fading channels with shadowing ((2,2,3,3) symmetric scenario).

Four schemes are simulated: (1) conventional single-user detector(5); (2) the optimal multiuser receiver in [8]; (3) JT-decomp (26) with precompensation; (4) JT-decomp without precompensation. Identical power constraint for each BS is assumed, with transmit SNR of 25 dB at each BS. Note that due to the path loss, the received SNR associated with the in-cell signal for MS at the cell borders will be weak and comparable with the interfering signals. For conventional

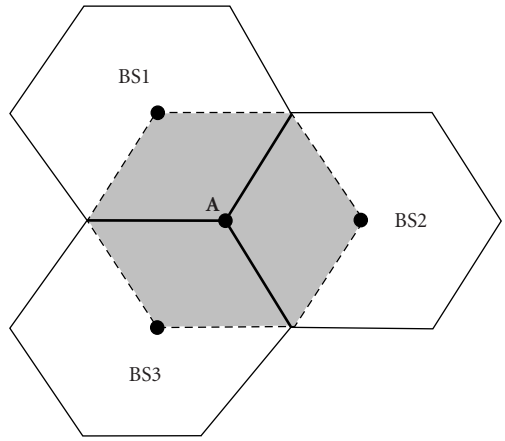


Figure 5: A realistic three-cell scenario.

single-cell signaling schemes (schemes (1) and (2)), a mobile user selects its associated BS with the largest path gain including the shadowing effect, and the power constraint at each BS is equally allocated to the in-cell users; while for the other two BS cooperation schemes, we use (20)–(21) to realize the power allocation. In scheme (4), with synchronization concerns, if $d_{b,j} - d_{b_j,j} < \Delta$, which corresponds to the case when user $j$ is located around point **A** or the cell borders (bold solid lines) in Figure 5, we can add BS $b$ to the BS set of MS $j$ denoted as $\boldsymbol{\beta}_j$. We assume that signals transmitted from BSs in $\boldsymbol{\beta}_j$ can be synchronously received at MS $j$, so JT-decomp is applied only if more than one user have the same BS set. Otherwise, single-user eigenbeamforming at cooperative BSs within $\boldsymbol{\beta}_j$ is implemented. On the other hand, joint transmission can always be conducted regardless of MS locations for scheme (3). Also for comparison, an interference-free scenario is drawn with the same per-user power as in schemes (1) and (2), which unrealistically assumes that the signals for three users each with single-cell signaling are orthogonal so that they do not interfere with each other, and the per-user rate is similar to (6).

Figure 6 shows the cumulative distribution functions (CDF) of the throughput for these schemes. We can find that the advantage of BS cooperation (scheme (3)) is still significant, although reduced a little from the strong CCI case in Figure 2. scheme (3) performs worse than the interference-free case because of its transmit power inefficiency. scheme (4) with $\Delta = 300$ m performs almost the same as scheme (2). Note that based on our parameter setting, for most of the cases, JT-decomp cannot be implemented. However, in practical urban cellular systems, where $N_t$ is much larger than $N_r$ and more users can be processed simultaneously, the chance of BS cooperation will get larger, so it is expected that scheme (4) will perform much better. Given the above analysis, together with the fact that scheme (2) is not practical for MS, joint transmission without precompensation still assumes substantial advantages over single-cell signaling schemes.

For comparison, we assume another case in which three users are uniformly distributed within 500 m around point **A** in Figure 5. In this scenario, average CCI becomes much stronger and BS cooperation can be applied with a much higher chance for scheme (4), resulting in the prominent performance gain of scheme (4) over scheme (2), as shown in Figure 7. Note that scheme (3) now outperforms the interference-free case because of the increased power gain, as discussed in Section 4.1. From the above observations, as joint transmission is most beneficial for strong CCI scenario, in reality, we can assign different sets of channels to near users (e.g., within 500 m of a BS) and far users (beyond 500 m), so they do not interfere with each other. We apply joint transmission only to the far cochannel users and go back to traditional transmission and detection for the near users. This scheme is especially applicable for indoor wireless access, which does not involve much mobility.

Therefore, we can conclude that BS cooperation schemes, either with or without precompensations, exhibit great advantage over single-cell schemes in realistic cellular applications, especially when CCI is strong.

## 7. CONCLUSIONS

In this paper, cooperative processing at multicell BSs is introduced to address problems inherent on the downlink of cellular multiuser MIMO communications. In particular, the capability for CCI cancellation, power gain, channel rank/conditioning advantage, and macrodiversity protection for BS cooperation are illustrated and verified. Although these advantages may not be achieved simultaneously and may compete with each other, there is still an optimistic prediction on the overall system performance improvement, which reveals the great potential of BS cooperative processing on meeting the ever-increasing capacity demands for wireless communications.

## APPENDICES

### A. EXTENSION OF LP-DP APPROACH IN [13] TO MULTICELL MIMO VECTOR BC SCENARIO

If $K = N_b$, with the LQ decomposition of $\mathbf{H}_T$,

$$\mathbf{H}_T = \begin{bmatrix} \mathbf{H}_{E1} \\ \mathbf{H}_{E2} \\ \vdots \\ \mathbf{H}_{EK} \end{bmatrix} = \mathbf{LQ} = \begin{bmatrix} \mathbf{L}_{1,1} & & & \\ \mathbf{L}_{1,2} & \mathbf{L}_{2,2} & \cdots & \\ \vdots & \cdots & \ddots & \cdots \\ \mathbf{L}_{1,N_b} & \cdots & \cdots & \mathbf{L}_{N_b,N_b} \end{bmatrix} \mathbf{Q}, \quad \text{(A.1)}$$

where $\mathbf{L}$ is lower triangular and $\mathbf{Q}$ is unitary, and each block $\mathbf{L}_{i,j}$ is an $N_r \times N_t$ submatrix. We can get

$$\mathbf{H}_{Ej} = [\mathbf{L}_{1,j}, \mathbf{L}_{2,j}, \ldots, \mathbf{L}_{j,j}, \mathbf{0}, \ldots, \mathbf{0}]\mathbf{Q}. \quad \text{(A.2)}$$

By defining $\mathbf{v} = \mathbf{QTs}_{[j]} = [\mathbf{v}_1^T, \mathbf{v}_2^T, \ldots, \mathbf{v}_K^T]^T$, (4) can be rewritten as a virtual vector BC:

$$\mathbf{y}_j = [\mathbf{L}_{1,j}, \mathbf{L}_{2,j}, \ldots, \mathbf{L}_{j,j}, \mathbf{0}, \ldots, \mathbf{0}]\mathbf{v} + \mathbf{n}_j, \quad \text{(A.3)}$$

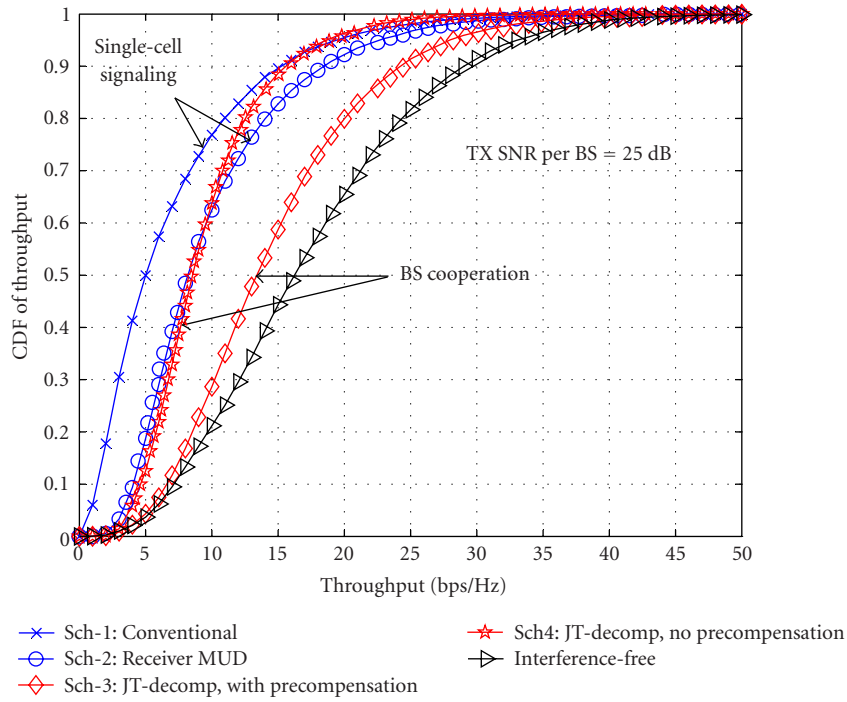


Figure 6: CDFs of schemes (1)–(4) for users uniformly located in the shadowed area of Figure 5.

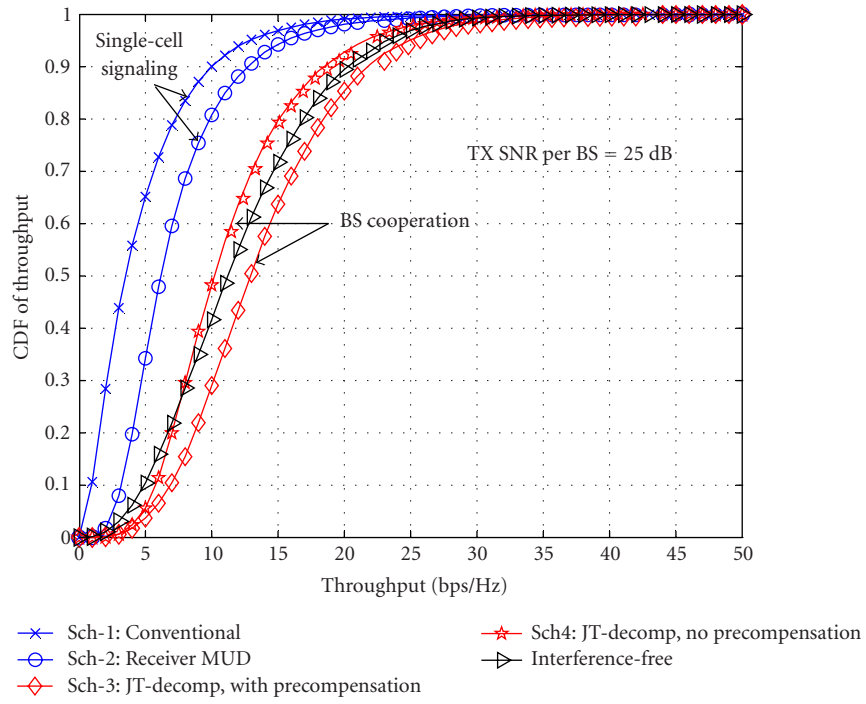


Figure 7: CDFs of schemes (1)–(4) for users uniformly located within 500 m of point **A** in Figure 5.

where submatrix $\mathbf{L}_{j,j}$ represents the virtual channel matrix through which virtual signal $\mathbf{v}_j$ is transmitted to MS $j$; and $\mathbf{L}_{i,j}$ represents the virtual interfering channel matrix from "previous" users. With DPC, if the encoder of user $j$ knows the noncausal virtual sequences of interference from user 1 to $j-1$, the mutual information for user $k$ is the same as if

the interference does not exist at all [14]. Then we can get $K$ virtual parallel and noninterfering subchannels as

$$\mathbf{y}_j = \mathbf{L}_{j,j}\mathbf{v}_j + \mathbf{n}_j, \quad 1 \le j \le K. \tag{A.4}$$

Each such virtual channel can be further decomposed into parallel substreams by SVD: $\mathbf{L}_{j,j} = \mathbf{U}_j\mathbf{\Sigma}_j\mathbf{V}_j^H$. With a similar approach as (13), the joint transmission matrix can be expressed as

$$\begin{aligned}\mathbf{T}\mathbf{s}_{[j]} &= \mathbf{Q}^H\mathbf{v} \\ &= \mathbf{Q}^H\begin{bmatrix}\mathbf{V}_1\mathbf{\Lambda}_1\mathbf{s}'_{1\_j}\\ \mathbf{V}_2\mathbf{\Lambda}_2\mathbf{s}'_{2\_j}\\ \vdots\\ \mathbf{V}_j\mathbf{\Lambda}_j\mathbf{s}_j\\ \vdots\\ \mathbf{V}_{N_b}\mathbf{\Lambda}_{N_b}\mathbf{s}'_{K\_j}\end{bmatrix} \Longrightarrow \mathbf{T} \\ &= \mathbf{Q}^H\begin{bmatrix}\mathbf{V}_1\mathbf{\Lambda}_1 & 0 & \cdots & 0\\ 0 & \cdots & \vdots & \vdots\\ 0 & \cdots & \cdots & \mathbf{V}_{N_b}\mathbf{\Lambda}_{N_b}\end{bmatrix}.\end{aligned} \tag{A.5}$$

The sum rate achieved by LP-DP is then given as in (21):

$$\mathrm{SR}_{\text{LP-DP}} = \sum_{j=1}^{K}\sum_{l=1}^{L_j}\log\left|1+\frac{P_{j,l}\lambda_{j,l}^2}{N_0}\right|, \tag{A.6}$$

where $\lambda_{j,l}$ represents the $l$th nonzero singular value of the virtual channel $\mathbf{L}_{j,j}$, and $P_{j,l}$ can be the result of water filling or equal power allocation.

## B. THE APPROXIMATE 2 BPS/HZ POWER GAIN IN FIGURE 2

We can compare Sato's bound and single-cell upper bound at high SNR. Because $\mathbf{H}_T$ has full rank (rank = 6), for Sato's bound, the average per-user rate approximation at high SNR is

$$\begin{aligned}\frac{1}{K}\mathrm{SR}_{\text{Sato}} &= \frac{1}{K}\sum_{l=1}^{\mathrm{rank}(\mathbf{H}_T)}\log\left(1+\frac{P_l}{N_0}\lambda_l^2\right)\\ &\approx \frac{1}{K}\sum_{l=1}^{\mathrm{rank}(\mathbf{H}_T)}\log\left(\frac{P_l}{N_0}\lambda_{T\_l}^2\right)\\ &= \frac{\mathrm{rank}\,(\mathbf{H}_T)}{K}\log\left(\frac{P_t}{\mathrm{rank}\,(\mathbf{H}_T)N_0}\right)\\ &\quad+\frac{1}{K}\sum_{l=1}^{\mathrm{rank}(\mathbf{H}_T)}\log\left(\lambda_{T\_l}^2\right).\end{aligned} \tag{B.1}$$

Similarly, the per-user rate for single-cell upper bound is

$$\begin{aligned}R_{1\_\text{single cell}} &= \sum_{l=1}^{\mathrm{rank}(\mathbf{H}_{b_1,1})}\log\left(1+\frac{P_l}{N_0}\lambda_{1\_l}^2\right)\\ &\approx \sum_{l=1}^{\mathrm{rank}(\mathbf{H}_{b_1,1})}\log\left(\frac{P_l}{N_0}\lambda_{1\_l}^2\right)\\ &= \mathrm{rank}\,(\mathbf{H}_{b_1,1})\log\left(\frac{P}{\mathrm{rank}(\mathbf{H}_{b_1,1})N_0}\right)\\ &\quad+\sum_{l=1}^{\mathrm{rank}(\mathbf{H}_{b_1,1})}\log\left(\lambda_{1\_l}^2\right).\end{aligned} \tag{B.2}$$

We have $\mathrm{rank}(\mathbf{H}_{b_1,1}) = 2$, $\mathrm{rank}(\mathbf{H}_T) = 6$, $K = 3$, and $P_t = 3P$ in our simulation. Therefore, the first summands in (B.1) and (B.2) are equal, and the gap between them is then

$$\begin{aligned}&\frac{1}{K}\mathrm{SR}_{\text{Sato}} - R_{1\_\text{single cell}}\\ &\quad= \frac{1}{K}\sum_{l=1}^{\mathrm{rank}(\mathbf{H}_T)}\log\left(\lambda_l^2\right) - \sum_{l=1}^{\mathrm{rank}(\mathbf{H}_{b_1,1})}\log\left(\lambda_l^2\right)\\ &\quad\sim \frac{1}{K}\mathrm{rank}\,(\mathbf{H}_T)\log\left(\frac{1}{\mathrm{rank}\,(\mathbf{H}_T)}\sum_{l=1}^{\mathrm{rank}(\mathbf{H}_T)}\lambda_{T\_l}^2\right)\\ &\qquad-\mathrm{rank}\,(\mathbf{H}_{b_1,1})\log\left(\frac{1}{\mathrm{rank}\,(\mathbf{H}_{b_1,1})}\sum_{l=1}^{\mathrm{rank}(\mathbf{H}_{b_1,1})}\lambda_{1\_l}^2\right)\\ &\quad= 2\log\left(\frac{24}{6}\right) - 2\log\left(\frac{4}{2}\right) = 2\,\text{bps/Hz},\end{aligned} \tag{B.3}$$

given $E(\sum_{l=1}^{\mathrm{rank}(\mathbf{H}_T)}\lambda_{T\_l}^2) = E(\|\mathbf{H}_T\|_F^2) = 24$, $E(\sum_{l=1}^{\mathrm{rank}(\mathbf{H}_{b_1,1})}\lambda_{1\_l}^2) = E(\|\mathbf{H}_{b_1,1}\|_F^2) = 4$ based on our parameter setting.

## REFERENCES


[1] G. J. Foschini and M. J. Gans, "On limits of wireless communications in a fading environment when using multiple antennas," *Wireless Personal Communications*, vol. 6, no. 3, pp. 311–335, 1998.

[2] A. Goldsmith, S. A. Jafar, N. Jindal, and S. Vishwanath, "Capacity limits of MIMO channels," *IEEE Journal on Selected Areas in Communications*, vol. 21, no. 5, pp. 684–702, 2003.

[3] S. Catreux, P. F. Driessen, and L. J. Greenstein, "Simulation results for an interference-limited multiple-input multiple-output cellular system," *IEEE Communications Letters*, vol. 4, no. 11, pp. 334–336, 2000.

[4] M. T. Ivrlac, W. Utschick, and J. A. Nossek, "Fading correlations in wireless MIMO communication systems," *IEEE Journal on Selected Areas in Communications*, vol. 21, no. 5, pp. 819–828, 2003.

[5] D.-S. Shiu, G. J. Foschini, M. J. Gans, and J. M. Kahn, "Fading correlation and its effect on the capacity of multielement antenna systems," *IEEE Trans. Communications*, vol. 48, no. 3, pp. 502–513, 2000.

[6] D. Chizhik, G. J. Foschini, M. J. Gans, and R. A. Valenzuela, "Keyholes, correlations, and capacities of multielement transmit and receive antennas," *IEEE Transactions on Wireless Communications*, vol. 1, no. 2, pp. 361–368, 2002.

[7] R. S. Blum, J. H. Winters, and N. Sollenberger, "On the capacity of cellular systems with MIMO," in *Proc. Fall IEEE 54th Vehicular Technology Conference (VTC '01)*, vol. 2, pp. 1220–1224, Atlantic City, NJ, USA, October 2001.

[8] H. Dai and H. V. Poor, "Asymptotic spectral efficiency of multicell MIMO systems with frequency-flat fading," *IEEE Trans. Signal Processing*, vol. 51, no. 11, pp. 2976–2988, 2003.

[9] H. Dai, A. F. Molisch, and H. V. Poor, "Downlink capacity of interference-limited MIMO systems with joint detection," *IEEE Transactions on Wireless Communications*, vol. 3, no. 2, pp. 442–453, 2004.

[10] P. W. Baier, M. Meurer, T. Weber, and H. Troger, "Joint transmission (JT), an alternative rationale for the downlink of time division CDMA using multi-element transmit antennas," in *Proc. IEEE 6th International Symposium on Spread Spectrum Techniques and Applications (ISSSTA '00)*, vol. 1, pp. 1–5, Parsippany, NJ, USA, September 2000.

[11] R. F. H. Fischer, C. Windpassinger, A. Lampe, and J. B. Huber, "MIMO precoding for decentralized receivers," in *Proc. IEEE International Symposium on Information Theory (ISIT '02)*, p. 496, Palais de Beaulieu, Lausanne, Switzerland, June–July 2002.

[12] K.-K. Wong, R. D. Murch, R. S.-K. Cheng, and K. B. Letaief, "Optimizing the spectral efficiency of multiuser MIMO smart antenna systems," in *Proc. IEEE Wireless Communications and Networking Conference (WCNC '00)*, vol. 1, pp. 426–430, Chicago, Ill, USA, September 2000.

[13] S. Shamai and B. M. Zaidel, "Enhancing the cellular downlink capacity via co-processing at the transmitting end," in *Proc. Spring IEEE 53rd Vehicular Technology Conference (VTC '01)*, vol. 3, pp. 1745–1749, Rhodes, Greece, May 2001.

[14] M. Costa, "Writing on dirty paper," *IEEE Transactions on Information Theory*, vol. 29, no. 3, pp. 439–441, 1983.

[15] S. Verdu, *Multiuser Detection*, Cambridge University Press, Cambridge, UK, 1998.

[16] N. Jindal, S. Vishwanath, and A. Goldsmith, "On the duality of Gaussian multiple-access and broadcast channels," in *Proc. IEEE International Symposium on Information Theory (ISIT '02)*, p. 500, Palais de Beaulieu, Lausanne, Switzerland, June–July 2002.

[17] N. Jindal, S. A. Jafar, S. Vishwanath, and A. Goldsmith, "Sum power iterative water-filling for multi-antenna Gaussian broadcast channels," in *Proc. Conference Record of the 36th Asilomar Conference on Signals, Systems, and Computers (Asilomar '02)*, vol. 2, pp. 1518–1522, Pacific Grove, Calif, USA, November 2002.

[18] W. Yu, "A dual decomposition approach to the sum power Gaussian vector multiple access channel sum capacity problem," in *Proc. IEEE 37th Annual Conference on Information Sciences and Systems (CISS '03)*, Johns Hopkins University, Baltimore, Md, USA, March 2003.

[19] W. Yu, W. Rhee, S. Boyd, and J. M. Ciofli, "Iterative water-filling for Gaussian vector multiple access channels," in *Proc. IEEE International Symposium on Information Theory (ISIT '01)*, p. 322, Washington, DC, USA, June 2001.

[20] H. Sato, "An outer bound to the capacity region of broadcast channels," *IEEE Transactions on Information Theory*, vol. 24, no. 3, pp. 374–377, 1978.

[21] G. Caire and S. Shamai, "On the achievable throughput of a multiantenna Gaussian broadcast channel," *IEEE Transactions on Information Theory*, vol. 49, no. 7, pp. 1691–1706, 2003.

[22] S. A. Jafar, G. J. Foschini, and A. J. Goldsmith, "PhantomNet: exploring optimal multicellular multiple antenna systems," in *Proc. Fall IEEE 56th Vehicular Technology Conference (VTC '02)*, vol. 1, pp. 261–265, Vancouver, BC, Canada, September 2002.

[23] S. A. Jafar and A. J. Goldsmith, "Transmitter optimization for multiple antenna cellular systems," in *Proc. IEEE International Symposium on Information Theory (ISIT '02)*, p. 50, Palais de Beaulieu, Lausanne, Switzerland, June–July 2002.

[24] R. Choi and R. Murch, "MIMO transmit optimization for wireless communication systems," in *Proc. 1st IEEE International Workshop on Electronic Design, Test and Applications (DELTA '02)*, pp. 33–37, Christchurch, New Zealand, January 2002.

[25] Q. H. Spencer and M. Haardt, "Capacity and downlink transmission algorithms for a multi-user MIMO channel," in *Proc. Conference Record of the 36th Asilomar Conference on Signals, Systems, and Computers (Asilomar '02)*, vol. 2, pp. 1384–1388, Pacific Grove, Calif, USA, November 2002.

[26] A. D. Wyner, "Shannon-theoretic approach to a Gaussian cellular multiple-access channel," *IEEE Transactions on Information Theory*, vol. 40, no. 6, pp. 1713–1727, 1994.

[27] T. S. Rappaport, *Wireless Communications: Principles and Practice*, Prentice-Hall, Englewood Cliffs, NJ, USA, 1996.

**Hongyuan Zhang** received the B.E. degree in electrical engineering from Tsinghua University, Beijing, China, in 1998, and the M.S. degree in electrical engineering from Chinese Academy of Sciences, Beijing, China, in 2001. He is currently pursuing the Ph.D. degree at the Department of Electrical and Computer Engineering, NC State University, Raleigh, NC. His current interests are in the areas of wireless communications, information theory, multiple user systems, and multi-input multi-output (MIMO) antenna systems.

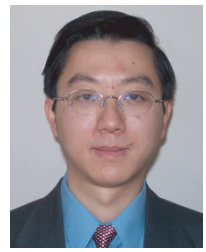

**Huaiyu Dai** received the B.E. and M.S. degrees in electrical engineering from Tsinghua University, Beijing, China, in 1996 and 1998, respectively, and the Ph.D. degree in electrical engineering from Princeton University, Princeton, NJ, in 2002. He worked at Bell Labs, Lucent Technologies, Holmdel, NJ, during the summer of 2000, and at AT&T Labs-Research, Middletown, NJ, during the summer of 2001. Currently, he is an Assistant Professor of electrical and computer engineering at NC State University. His research interests are in the general areas of communication systems and networks, advanced signal processing for digital communications, and communication theory and information theory. He has worked in the areas of digital communication system design, speech coding and enhancement, and DSL transmission. His current research focuses on space-time communications and signal processing, the turbo principle and its applications, multiuser detection, and the information-theoretic aspects of multiuser communications and networks.